Journal of Molecular Catalysis A: Chemical 323 (2010) 84–90

Contents lists available at ScienceDirect

Journal of Molecular Catalysis A: Chemical

journal homepage: www.elsevier.com/locate/molcata

Alumina-supported iron oxide nanoparticles as Fischer–Tropsch catalysts: Effect of particle size of iron oxide

Jo-Yong Park[a,b], Yun-Jo Lee[a,*], Pawan K. Khanna[a,c], Ki-Won Jun[a,**], Jong Wook Bae[a], Young Ho Kim[b]

[a] Petroleum Displacement Technology Research Center, Korea Research Institute of Chemical Technology (KRICT), P.O. BOX 107, Yuseong, Daejeon 305-600, Republic of Korea
[b] Department of Fine Chemical Engineering and Applied Chemistry, BK21-E2M, Chungnam National University, Daejeon 305-764, Republic of Korea
[c] Nanoscience Laboratory, Centre for Materials for Electronics Technology (C-MET), Panchwati, off Pashan Road, Pune 411 008, India

ARTICLE INFO

Article history:
Received 14 January 2010
Received in revised form 15 March 2010
Accepted 20 March 2010
Available online 27 March 2010

Keywords:
Fe/Al_2O_3 catalyst
Size-defined nanoparticle
Fischer–Tropsch synthesis

ABSTRACT

The Fischer–Tropsch synthesis of unpromoted and nano-sized iron oxide supported on δ-Al_2O_3 was investigated using a fixed-bed reactor. The catalysts prepared from pre-synthesized iron oxide with varying particle size (2–12 nm) showed much higher catalytic activities than the one prepared by using conventional impregnation method. The best results for CO conversion were obtained when the catalyst had Fe particle size of 6.1 nm. With an increase in particle size, the reduction degree and C_5+ selectivity was increased, whereas CH_4 selectivity and the uptake of adsorbed CO were decreased. Turnover frequency (TOF) at 300 °C was increased from 0.02 to 0.16 s^{-1} when $d(Fe^0)$ was increased from 2.4 to 6.2 nm, and then it remains almost constant up to a particle size of 11.5 nm. Particle sizes of prepared iron oxide were analyzed by XRD and TEM, and the reduction behaviors of Fe/Al_2O_3 catalysts were studied by H_2-TPR. The effective iron size, metal dispersion and reduction degree of Fe/Al_2O_3 catalysts were measured by CO chemisorption and O_2 titration.

1. Introduction

In recent years, the catalytic activity of the materials has been reported to be dependent on the particle size and is considered as one of the main factors that affects the catalytic activity and selectivity during Fischer–Tropsch Synthesis (FTS). Many researchers [1–13] have studied the size effect of cobalt metal in FT catalyst. While turnover frequency (TOF) depends on cobalt particle size for smaller size (<8 nm), it is independent of the particle size for bigger size (>8 nm) [1].

Iron-based FT catalysts have not much persuaded particularly with respect to the particle size effect [14,15]. Mabaso et al. reported the effect of crystal size on carbon supported iron catalysts prepared via precipitation using reverse micelle systems where catalysts with smaller metal than 7–9 nm have showed lower TOF and higher selectivity of methane compared to the bigger-sized catalysts [14]. Although recently a good account of reaction mechanism for FTS using iron catalysts have been documented by Davis [4,5]. It has been suggested that pre-reduced metallic iron is mostly changed to iron oxide surrounded by an iron carbide layer in bulk composition under FTS reaction condition [16]. The iron carbides are considered as a catalytic active phase [17].

Usually Fe-based FT catalysts have been prepared by the conventional methods, i.e. impregnation or coprecipitation [15,18,19]. In such methods, it is difficult to control an iron crystal size in the catalysts where the crystal has broad distribution in particle size. Such unavoidable variations in the crystallite size of the catalyst may reduce catalytic efficiency because the catalytic activity is maximized in optimum crystal size in FTS reaction [14]. Furthermore a problem which often associates with these conventional methods is agglomeration of particles and sintering of active metal on the surface during the calcinations [20]. It has also been reported that in the supported iron catalyst it is very difficult to completely reduce the small-sized iron species due to strong metal–support interaction when the iron loading is lower than 10% [21,22].

It is well known that the agglomeration and sintering of iron-based catalyst may lead to low catalytic activity. This therefore, warrants some smart strategy for use of iron-based catalysts. One certain way to overcome these drawbacks, is to apply innovative synthesis of nanoparticles of the catalysts, e.g. nano-iron oxide particles that can be easily dispersed in organic medium and can be homogenously loaded on to the support materials.

In this paper, we present design and preparation of the size-defined Fe/Al_2O_3 catalyst using pre-synthesized γ-Fe_2O_3 nanoparticles. Catalysts based on such size-defined particles are expected to prevent the agglomeration of small particles by sintering of active metal. This may be possible because the pre-synthesized size-defined nanoparticles of iron oxide are dispersible and can be homogenously impregnated on the alumina support

* Corresponding author. Tel.: +82 42 860 7630; fax: +82 42 860 7388.
** Corresponding author. Tel.: +82 42 860 7671; fax: +82 42 860 7388.
E-mail addresses: yjlee@krict.re.kr (Y.-J. Lee), kwjun@krict.re.kr (K.-W. Jun).

1381-1169/$ – see front matter © 2010 Elsevier B.V. All rights reserved.
doi:10.1016/j.molcata.2010.03.025

and thus making them more active in FTS. We thus expect that the size-defined Fe/Al_2O_3 catalyst have better scope in activity and selectivity in FTS. In present work, a relationship between catalytic activity and crystal size of iron oxide is studied by using X-ray diffraction (XRD), transmission electron microscopy (TEM), H_2 temperature-programmed reduction (H_2-TPR), CO chemisorption and O_2 titration.

2. Experimental

2.1. Preparation of size-defined iron oxide (γ-Fe_2O_3)

Size-defined iron oxides were prepared by the solvothermal method. The detailed procedure of this method has been published elsewhere [23]. The iron-oleate precursor was synthesized from iron nitrate, oleic acid and NH_3 (30%) solution. The iron-oleate precursor was added in octadecene and then heated to 130–250 °C for 5 h. After cooling to room temperature, the resulting nanoparticles of iron oxide were collected after repeated washing with acetone and were then air-dried. Finally, the nanoparticles were dispersed in hexane. The nano-sized iron oxide samples are designated as *x*-Fe where *x* means reaction temperature in Celsius.

2.2. Catalyst preparation

Catalyst support was prepared by modification of our previous method [24]. γ-Al_2O_3 with high surface area (~350 m^2/g) was calcined at 1000 °C to prepare δ-Al_2O_3 support (surface area of 127 m^2/g) having less reactive surface. Supported catalysts of Fe/Al_2O_3 = 5/100 wt ratio (denoted to *x*-FeAl, *x* means the synthesis temperature of the nanoparticles) were prepared by impregnation of the pre-synthesized γ-Fe_2O_3 nanoparticles (*x*-Fe) solution dispersed in hexane. The prepared catalysts were dried at 60 °C for 12 h and then calcined at 400 °C for 5 h in static air. For comparison, the reference catalyst denoted to i-FeAl was also prepared by conventional impregnation method by homogenously mixing the δ-Al_2O_3 with iron nitrate in ethanol.

2.3. Activity test

Typically, 0.5 g of the Fe/Al_2O_3 catalyst was reduced in flowing 5% H_2/Ar (200 cm^3/min) at 450 °C for 12 h. FTS activities of the reduced catalysts were tested using a fixed-bed reactor. The activity tests were conducted under the following reaction conditions; T = 280–300 °C; Pg = 10 kgf/cm^2; SV (L/kg_{cat}/h) = 3600; feed compositions H_2/CO/Ar = 63.2/31.3/5.5; mol%.

2.4. Catalyst characterization

The catalysts processed from pre-synthesized γ-Fe_2O_3 nanoparticles or those obtained *via* impregnation method were studied by XRD measurement using a Rigaku D/MAX-2200V diffractometer with Cu/K-alpha radiation (λ = 0.154056 nm). TEM was performed with TECNAI G20 instrument for the study of the particle morphology and for obtaining exact particle size of iron oxide. TPR was recorded using a Micromeritics ASAP 2920 equipped with a thermal conductive detector (TCD). The samples were first pretreated in a helium flow up to 200 °C and kept for 2 h to remove the adsorbed water, and then cooling to 100 °C. The reducing gas containing 5% H_2/Ar mixture was passed over the samples at a flow rate of 30 cm^3/min. The samples were heated from 100 to 1000 °C with heating rate of 10 °C/min and kept at that temperature for 30 min. The number of active metal on the surface in the Fe-based catalyst was measured by CO chemisorption at 35 °C in conventional volumetric adsorption system using micrometrics ASAP 2020C instrument. The sample (0.1 g) was reduced in situ at 450 °C for 12 h under flowing H_2, and then the gas was changed to He flow and cooled to 35 °C. The CO chemisorption was carried out at 35 °C. A Fe: CO stoichiometry is assumed to 2:1. After CO chemisorption measurement, the sample was re-oxidized at 450 °C by 10% O_2 in helium to determine the extent of reduction. Dispersion percentage (*D*%) of the iron metal was calculated according to the equation as has been described in the literature [15,18].

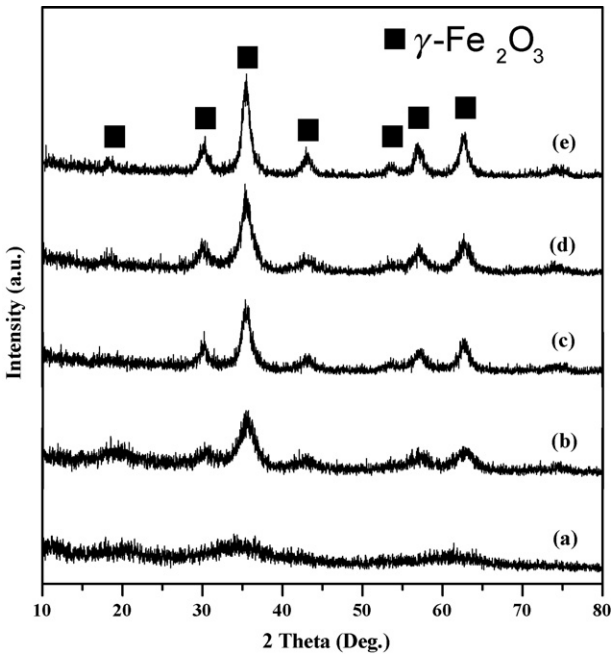

Fig. 1. X-ray diffraction patterns of the size-defined iron oxide: (a) 130-Fe, (b) 180-Fe, (c) 200-Fe, (d) 230-Fe, (e) 250-Fe.

$$D\% = \frac{1.117X}{Wf}$$

where X (μ mol/g) is the total CO uptake, W is the weight percentage of iron, and f is the fraction of iron reduced to the metal determined from O_2 titration. Average particle size (d_p (nm)) was calculated from *D*% assuming spherical metal crystallite of uniform diameter.

$$d_p = \frac{96}{D\%}$$

3. Results and discussion

3.1. Analysis of size-defined iron oxide

The crystal phase of the prepared iron oxide nanoparticles of varying size is studied using XRD pattern. Fig. 1(a)–(e) shows the XRD spectra of iron oxide prepared from iron-oleate precursor in octadecene at different temperatures, i.e. 130, 180, 200, 230 and 250 °C, respectively. The XRD patterns of so-obtained iron oxide reveals a face-centered cubic crystal structure which relates well with γ-Fe_2O_3 and all relevant diffraction peaks are well matched with the reported value for this product [25]. In the present study, the particle size can be varied by varying the reaction temperature. The distinguishable difference in the XRD patterns clearly indicates the temperature dependency of the nanoparticles. It is observed that on increasing reaction temperature, the particle size increases and the peaks become more prominent. Thus the XRD peaks for the product that was obtained at 130 °C is very shallow and poorly resolved, and the XRD pattern of the product synthesized at 250 °C shows well-defined Bragg's reflections, indicative of comparatively

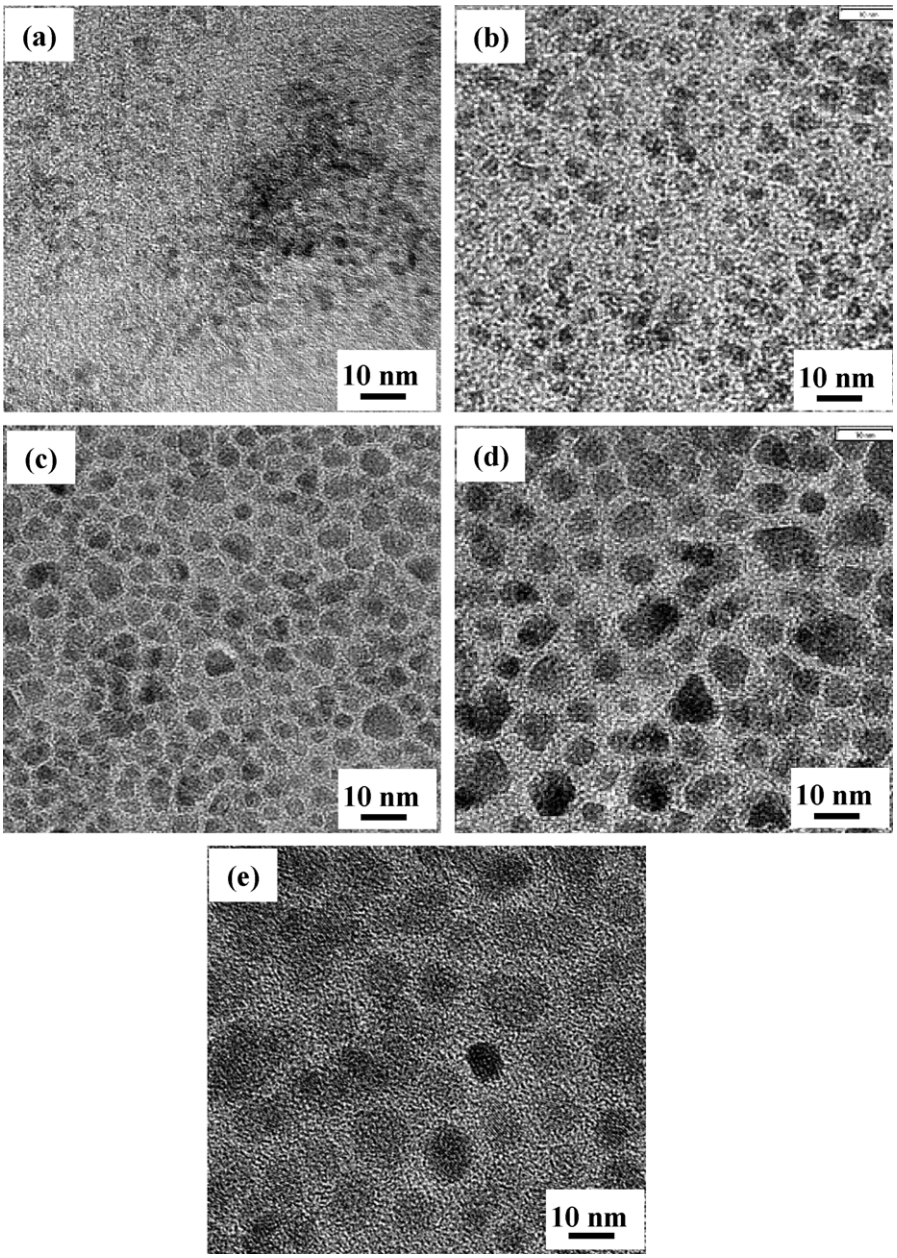

Fig. 2. TEM images of the size-defined iron oxide: (a) 130-Fe, (b) 180-Fe, (c) 200-Fe, (d) 230-Fe, (e) 250-Fe.

bigger particles. The crystallite size was calculated using Scherer's equation [26] taking diffraction peak at $2\theta = 36$ and is estimated to be between 2.0 and 12.4 nm (Table 1).

Fig. 2 shows TEM micrographs of prepared iron oxide nanoparticles. TEM images clearly indicate that most of the nanoparticles are spherical and uniform irrespective of their preparation temperature. Average particle size of iron oxide increases from about 2.0 to 12.0 nm with increasing the reaction temperature and this finding is similar to the results calculated from the XRD line broadening. The bigger particles are more uniform in their dimensions than the smaller particles simply because of no agglomeration due to presence of optimum surfactant amount around the nanoparticles. Also the preparation at higher temperature reveals that the particles are more crystalline and the lattice fringes can be seen from the TEM pictures in Fig. 2(e). Table 1 shows the comparison between the particles calculated from the XRD patterns and those obtained form TEM analysis.

Table 1
Particle size of the size-defined iron oxide (γ-Fe_2O_3).

Sample No.	Iron oxide particle size (nm)	
	XRD	TEM
130-Fe	<2.0	2.0
180-Fe	4.6	4.5
200-Fe	6.2	6.1
230-Fe	9.3	9.0
250-Fe	12.4	12.0

3.2. Analysis of Fe/Al_2O_3 catalysts derived from pre-synthesized γ-Fe_2O_3

Fig. 3 shows the XRD patterns of the supported and calcined Fe/Al_2O_3 catalysts. The broad peaks at 2θ values of 20.0, 31.1, 36.6, 39.3, 44.9, 59.9 and 67.3° are associated with δ-Al_2O_3 (marked with blank rectangles) [27]. Similarly, reflections at 2θ value of 24.1, 32.9,

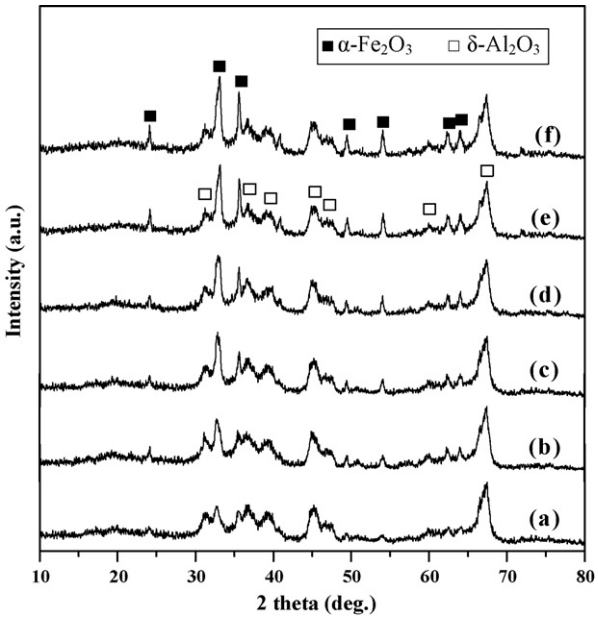

Fig. 3. XRD patterns of the size-defined Fe/Al_2O_3 catalysts: (a) δ-Al_2O_3 support, (b) 130-FeAl, (c) 180-FeAl, (d) 200-FeAl, (e) 230-FeAl, (f) 250-FeAl.

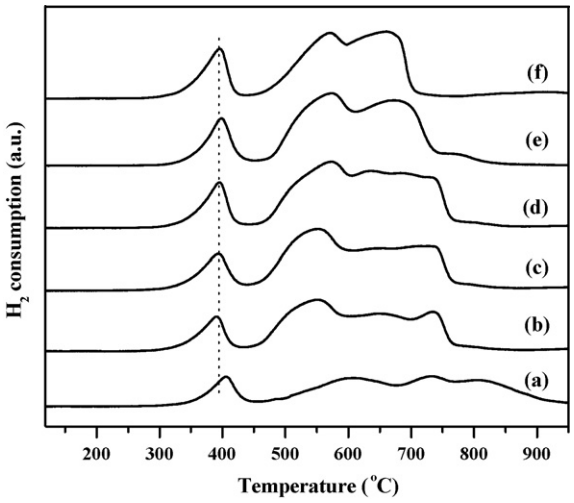

Fig. 5. H_2-TPR profiles of the size-defined Fe/Al_2O_3 catalysts: (a) i-FeAl, (b) 130-FeAl, (c) 180-FeAl, (d) 200-FeAl, (e) 230-FeAl, (f) 250-FeAl.

35.6, 40.8, 49.3, 54.0, 62.3 and 64.0° are due to α-Fe_2O_3 (marked as black rectangles) and match well with the reported data on hematite iron oxide [28]. It can be seen that some peaks for alumina and iron oxide are overlapped, and thus the accurate peak width of iron oxides is difficult to ascertain. After heating Fe/Al_2O_3 catalysts in air at 400 °C for 5 h, the color of the calcined Fe/Al_2O_3 catalysts was changed from black to red showing phase change from original maghemite (γ-Fe_2O_3) to final hematite (α-Fe_2O_3) which is consistent with the reported observation [15].

Similar to pre-synthesized iron oxide, an increase in peak intensity was observed with increasing particle size of the catalyst even after calcinations. Careful examination of the XRD pattern shows more intense and well-defined peaks for 250-FeAl catalyst as compared to that of 130-FeAl. Thus from XRD patterns, it is clear that the initial difference of particle size of iron oxide continues even when these have been loaded in support and calcined to temperature as high as 400 °C. In other words, the particle sizes of the iron oxide between in Fe/Al_2O_3 catalyst and in as-prepared γ-Fe_2O_3 are similar, which means that there is no significant agglomeration of iron oxide nanoparticles in Fe/Al_2O_3 after calcination.

Fig. 4 shows TEM images of δ-Al_2O_3 support and supported 200-FeAl catalyst. The alumina support has fiber-like morphology with particle size of 20–40 nm in length and 5–10 nm in width as shown in Fig. 4(a). The δ-Al_2O_3 was prepared by the calcinations of γ-Al_2O_3 at high temperature of 1000 °C to reduce the number of surface hydroxyl group and consequently to minimize metal–support interaction. Iron oxide nanoparticle on the supported 200-FeAl catalyst shows reasonably homogenous distribution on the δ-Al_2O_3 support and has spherical morphology.

TPR studies were performed using H_2 on the supported catalysts. Fig. 5 shows the TPR results for the Fe/Al_2O_3 catalysts with different sizes of iron oxide. The figure also shows TPR of the catalyst prepared by using impregnation method (i-FeAl). It is reported that when hematite iron oxide is brought under the reducing environment of hydrogen gas, it changes to magnetite form and then to iron monoxide. The further reduction of iron oxide also makes it possible to be converted to metallic iron as reported in the literature [4,5] and as published by us recently [12]. In the present case, the TPR patterns of Fe/Al_2O_3 catalysts exhibit two peaks at about 400 and 560 °C, and a broad reduction feature between 600 and 800 °C, indicating that the reduction process could occur in two stages similar to that has been described by others [4,5,12,19,29]. Thus based on the known fact the reduction of such loaded catalyst go through a two-stage reduction profile i.e. in the first-stage α-Fe_2O_3 is reduced to Fe_3O_4 at 400 °C which in the second-stage undergoes further reduction process to possibly form a mixture of FeO and Fe or the Fe alone at around 560 °C. Since the second-stage reduction occurs at higher temperature, it may be considered for conversion of the iron oxide into metallic iron. Such an observation has also been reported for promoted iron catalyst [4,5,12]. In case of silica supported iron catalyst, it has been reported that iron silicate [29] may form which hinders the complete reduction of the iron species. Thus, in the present case third-peak can be associated with iron oxide layer which contacts on the alumina surface [30]. As the particle size of iron oxide on the Fe/Al_2O_3 catalyst increases, the intensity and area of first reduction peak also tend to increase

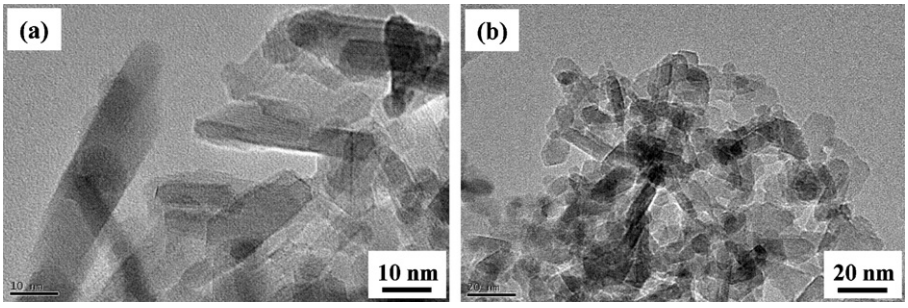

Fig. 4. TEM images of (a) δ-Al_2O_3 support and (b) supported 200-FeAl catalyst.

Table 2
Iron particle size as determined by CO chemisorption and O_2 titration of size-defined Fe/Al_2O_3 catalysts after reduction at 450 °C.

Sample	CO uptake (μ mol/g)	Uncorrected dispersion (%)[a]	Uncorrected Fe diameter (nm)[b]	O_2 uptake (μ mol/g)	Reduction degree (%)[c]	Corrected dispersion (%)[d]	Corrected Fe diameter (nm)[e]
i-FeAl	35.8	8.4	11.4	136	21.3	39.5	2.4
130-FeAl	31.9	7.5	12.8	142	22.2	33.7	2.8
180-FeAl	24.5	5.7	16.7	171	26.7	21.5	4.5
200-FeAl	20.7	4.9	19.8	202	31.6	15.4	6.2
230-FeAl	16.3	3.8	25.1	215	33.6	11.4	8.4
250-FeAl	13.2	3.1	31.0	238	37.2	8.3	11.5

[a] Dispersion (D) = surface Fe^0 atom/total Fe atom × 100, assumed stoichiometric adsorpton ratio of CO/Fe = 1/2.
[b] Fe particle size calculated from CO chemisorptions using $d(Fe) = 96/D$.
[c] Calculated from O_2 uptake.
[d] Corrected dispersion (D) = surface Fe^0 atom/total reduced Fe^0 atom × 100 = surface Fe^0 atom/(total Fe atom × reduced fraction) × 100.
[e] Corrected Fe diameter = uncorrected Fe diameter × reduced Fe fraction.

and shift to lower temperature. Also, the tail of third-peak moves to lower temperature with increasing particle size (Fig. 5(a)–(f)). The increased intensity of first and second peak suggests easy and more favored reduction for the bigger particle of Fe/Al_2O_3 catalyst within a size range of 2–12.0 nm (TEM). The formation of metallic iron may therefore be easier from the bigger particles. The presence of tail from the third-peak shows that the reduction of the small particles is difficult because of the fact that these particles with high surface area have reasonably strong interaction with the surfaces of alumina support thus hindering the reduction of the smaller particles that are strongly bound to alumina leading to formation of iron-aluminate at higher temperature. It is therefore appropriate to suggest that the different particle size lead to different reduction degree due to differences in their interaction with alumina. The TPR studies thus can be summarized as per the following equation:

$$Fe_2O_3 \rightarrow Fe_3O_4 \rightarrow FeO \rightarrow Fe \quad (1)$$

Chemisorption studies were performed using carbon monoxide gas which is useful for determination of the particle size for the reduced species. Table 2 shows the results of CO chemisorption and O_2 titration of the size-defined Fe/Al_2O_3 catalysts. High CO consumption is observed for the catalyst prepared by impregnation method, i.e. i-FeAl as well as for sample 130-FeAl compared to the catalysts that have bigger particles. The higher CO chemisorption therefore can mainly be considered because i-FeAl and 130-FeAl catalysts due to their small particle size, have higher dispersion and higher surface area of the metallic iron. The calculations of particle size from O_2 titration and CO chemisorptions show that the size of initial iron oxide estimated from XRD line broadening and TEM do not differ much from the final Fe/Al_2O_3 catalyst (Table 2). Particle size from this calculation is found to be between 2.4 nm (i-FeAl) and 11.5 nm (250-FeAl). Considering that the oxide shrinks to about 80% of the size of the original oxide when the nanoparticles of iron oxides are reduced to its metallic particles, the size of supported iron oxide calculated by the chemisorptions gives a little higher value especially in the case of smaller particles. Particle size of unsupported 130-Fe is 2.0 nm (TEM), but after loading the size of iron metal of 130-FeAl increases to 2.8 nm (chemisorptions). Whereas the size of 250-Fe with bigger particle just changes marginally from 12.0 nm (TEM) to 11.5 nm (chemisorptions). It means that smaller particles are more prone to be aggregated and sintered than bigger particles when it is loaded and calcined.

The O_2 titration results suggest different reduction degree for iron oxide on alumina. As the particle size of iron oxide increases, oxygen uptake also increases from initial 136 to 238 μmol/g_{cat}. The degree of reduction thus increases from 21.3% for i-FeAl to 37.2% for 250-FeAl with increasing particle size. The reduction degree of the i-FeAl was lower than that of all Fe/Al_2O_3 catalysts having nano-sized iron oxide (Table 2). Overall, the findings suggest that the oxygen uptake is inversely proportional to the CO uptake.

Table 3
CO conversion and product distribution at 280 °C.[a]

Sample No.	CO conversion (%)	Conversion of CO to CO_2 (%)	Hydrocarbon selectivity (%)		
			CH_4	C_2-C_4	C_5+
i-FeAl	5.8	1.2	25.0	38.5	36.5
130-FeAl	16.7	2.6	24.3	37.2	38.5
180-FeAl	25.3	4.4	19.2	35.6	45.2
200-FeAl	32.3	5.3	17.2	33.6	49.2
230-FeAl	21.7	3.2	14.3	31.1	54.6
250-FeAl	18.8	3.0	13.2	30.2	56.6

[a] Reaction conditions: T = 280 °C; Pg = 10 kgf/cm^2; SV (L/kg_{cat}/h) = 3600; feed compositions (H_2/CO/Ar = 63.2/31.3/5.5; mol%).

By comparing the O_2 titration of iron oxide on alumina support at different particle size, it can be seen that the reduction degree increases with increasing iron particle size. The low reduction degree of the i-FeAl catalyst can be attributed to the small iron oxide particle that can easily form iron–aluminate during calcinations or reduction process. Further the reduction of the iron–aluminate is extremely difficult and impractical at the adopted experimental temperature and therefore it is ineffective in the FTS. In addition, the size-defined Fe/Al_2O_3 catalyst prepared with small particle may also have strong metal–support interaction which suppresses the reducibility. Thus the degree of reduction is different for small particles and it has maximum value for bigger particles due to the fact that bigger particles have smaller contact area with the support, consequently resulting in more reducibility of iron oxide phase to iron metal. These results well coincide with TPR results of Fig. 5.

3.3. FTS performance

3.3.1. Conversion and selectivity

The size-defined Fe/Al_2O_3 catalysts were tested in a fixed-bed reactor at 280–300 °C at 10 bar under H_2/CO = 2 and GHSV = 3600 ml/(g_{cat} h). The catalytic activities with different particle size are shown in Tables 3 and 4. The trends of catalytic

Table 4
CO conversion and product distribution at 300 °C.[a]

Sample No.	CO conversion (%)	Conversion of CO to CO_2 (%)	Hydrocarbon selectivity (%)		
			CH_4	C_2-C_4	C_5+
i-FeAl	10.5	5.1	27.8	42.1	30.1
130-FeAl	24.7	7.5	26.1	39.0	34.9
180-FeAl	36.2	11.8	24.2	38.6	37.2
200-FeAl	47.8	13.1	22.9	37.3	39.8
230-FeAl	32.6	9.4	20.2	34.7	45.1
250-FeAl	28.1	8.3	18.1	33.1	48.8

[a] Reaction conditions: T = 300 °C; Pg = 10 kgf/cm^2; SV (L/kg_{cat}/h) = 3600; feed compositions (H_2/CO/Ar = 63.2/31.3/5.5; mol%).

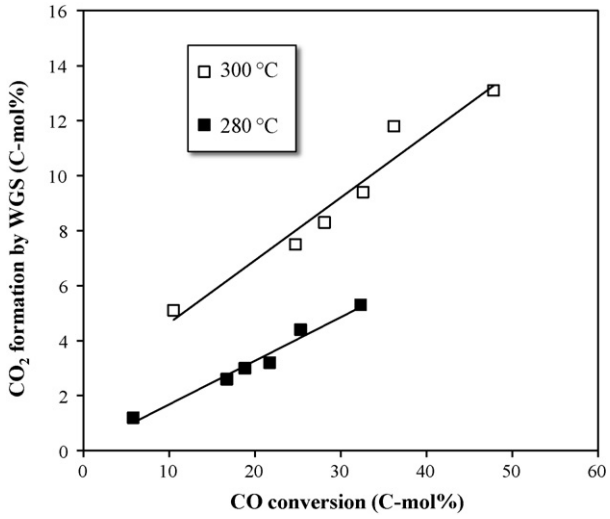

Fig. 6. Conversion of CO to CO_2 by WGS reaction on size-defined Fe/Al_2O_3 catalyst: reaction temperature = 280 and 300 °C, Pg = 10 kgf/cm^2; SV (L/kg$_{cat}$/h) = 3600; feed compositions (H_2/CO/Ar = 63.2/31.3/5.5; mol%).

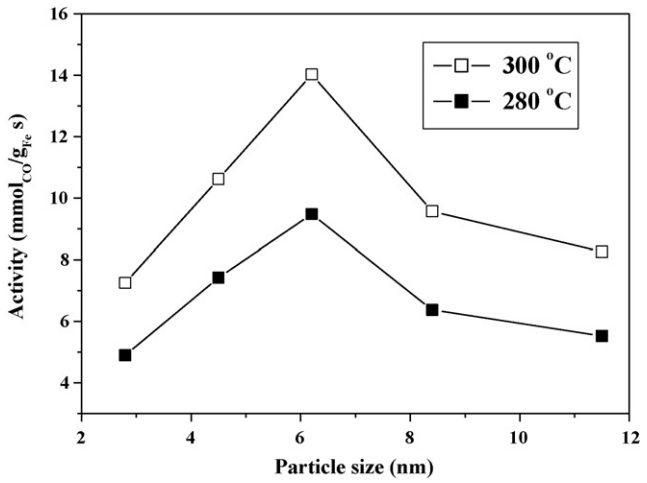

Fig. 7. The influence of iron particle size on size-defined Fe/Al_2O_3 catalyst. Reaction conditions: T = 280 and 300 °C; Pg = 10 kgf/cm^2; SV (L/kg$_{cat}$/h) = 3600; feed compositions (H_2/CO/Ar = 63.2/31.3/5.5; mol%).

performance of the Fe/Al_2O_3 catalysts at 280 °C are similar to results obtained at 300 °C. The CO conversion of Fe/Al_2O_3 catalyst is clearly seen to increase with increasing particle size of iron oxide in the range of between 2.0 and 6.1 nm. On the contrary, the CO conversion decreased with increasing the size of iron oxide from 6.1 to 12.0 nm. It can be seen from Tables 3 and 4 that by increasing the particle size from 2.0 to 6.1 nm, the CO conversion of catalyst increases from 16.7 to 32.3% at 280 °C and from 24.7 to 47.8% at 300 °C, respectively, and it appears that best catalytic activity can be attained with particle diameter of 6.1 nm. Both, the CO conversion and CO_2 selectivity follow the same trends due to water gas shift (WGS) reaction as shown in Fig. 6. Formation rate of CO_2 by WGS reaction is linearly correlated with CO conversion because FT reaction of every CO molecule produces a water molecule. It is well known that magnetite (Fe_3O_4) sites in iron-based FT catalyst are the most active phase for WGS reaction [31]. However, its rate is promoted at high temperature of 300 °C due to reaction kinetic control.

CH_4 and C_2-C_4 selectivity of Fe/Al_2O_3 catalyst decreases with increasing particle size from 2.0 to 12.0 nm in other words, C_5+ selectivity increases with increasing particle size. The catalyst with high CH_4 selectivity indicates that dissociated hydrogen is present on the catalyst surface. Because catalyst with smaller particle size has higher tendency to get hydrogen adsorption rather than dissociative adsorption of CO, they lead to increase population of hydrogen species at the surface. The large number of hydrogen species thus present on the surface is hydrogenated to CH_4 or light hydrocarbons [1,2,32]. The increasing C_5+ selectivity with increasing particle size of iron oxide could be due to easy activation and fast movement resulting in easy reaction with the adsorbed CO molecules. Under similar catalytic condition, the impregnated Fe catalyst (i-FeAl) show five times lower activity than best Fe catalyst, i.e. 200-FeAl. Such an observation hints towards a definite size-dependent FTS where the particle size of 6.1 nm is most suited for effective metal support interaction leading to efficient production of hydrocarbon. Particle smaller than this dimension shows low activity from the fact that their interaction with the support is so strong that they exist as oxide on the surface of support and part of the particles only exist as iron carbide in main and metallic state in part, and thus eventually losing their active sites. Furthermore smaller metal particles with high surface energy are apt to be oxidized by water produced during the FTS reaction [33]. The loss of active sites therefore leads to suppression of catalytic activity in i-FeAl catalyst because of much smaller size of iron. Since the difference in catalytic activity between size-defined catalyst and i-FeAl catalyst is large, it can be easily concluded that the particle size of iron oxide has great influence on the interaction between iron oxide and Al_2O_3, and on the reduction/carburization and the activity of catalysts. The catalytic performances of size-defined Fe/Al_2O_3 catalyst are in agreement with the results of CO chemisorption. To further verify such difference in the activity and their size dependency, specific activity is plotted versus the iron particle size (from chemisorption). Fig. 7 shows that when the iron particle size increases from 2.0 (130-FeAl) to 6.1 nm (200-FeAl), the activity increases rapidly due to improved reduction degree while the activity from 6.1 nm (200-FeAl) to 12.0 nm (250-FeAl) decrease due to the reduced surface area of Fe metal.

In Co-based FT catalysts, it has been reported that very small crystallites of Co (<6 nm) have low activity per unit metal site and high methane selectivity due to structure sensitivity of FT reaction [1,2]. Therefore in iron-based FT catalysts, a similar behavior might be expected.

3.3.2. *Turnover frequency (TOF)*

Since intrinsic activity may be related to the particle size, especially in FTS reaction, the correlation between TOF and iron particle size can be a useful way to understand the catalyst efficiency. The TOF is calculated using the dispersion obtained CO chemisorption and O_2 titration. The TOF data gathered at 280 and 300 °C based on the particle size are plotted as shown in Fig. 8. The TOF increases rapidly from 0.06 to 0.187 s^{-1} at 300 °C with the increase of the iron particle sizes in the range of between 2.0 and 6.1 nm and thereafter, it almost remains constant for the particles ranging from 6.1 to 12.0 nm. It is noteworthy that the TOF of the most active, 200-FeAl catalyst is 8 times higher than that of i-FeAl (0.023 s^{-1} at 300 °C) catalyst. This result shows that the size-defined Fe/Al_2O_3 catalyst is more efficient and better suited for FTS than conventional catalyst. The initial increase in turnover frequency with increasing particle size up to about 6.1 nm could be due to the presence of optimum active metal content on the surface but after this size domain, the effect is not so-prominent and the TOF is more or less unaffected by particle size. These results well coincide with those of cobalt-based catalysts, where TOF showed a sharp decline below Co particle sizes of 6 nm [1,2]. It is probably due to the high activation energy of CO on small metal surface [34].

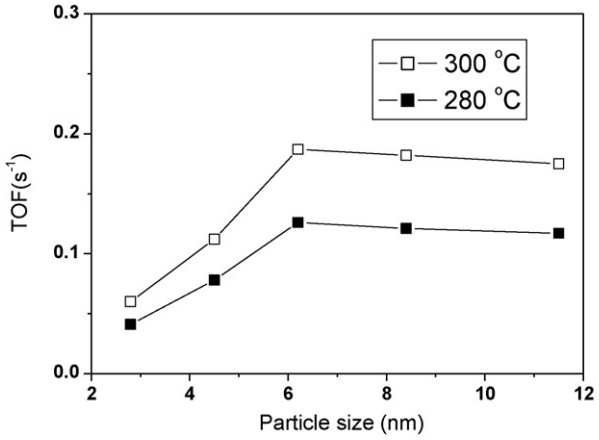

Fig. 8. The influence of iron particle size on the TOF. Reaction conditions: T = 280 and 300 °C; Pg = 10 kgf/cm^2; SV (L/kg$_{cat}$/h) = 3600; feed compositions (H_2/CO/Ar = 63.2/31.3/5.5; mol%).

4. Conclusions

The Fe/Al_2O_3 catalyst prepared from pre-synthesized and size-defined γ-Fe_2O_3 nanoparticles were investigated for the FTS. It is observed that small iron oxide particles lead to strong interactions between the support and the iron precursor which shift degree of reduction to higher temperature. Bigger iron oxide particles can be reduced easily due to weak interaction with the support but the bigger particles suppress the dispersion of iron oxide. Thus, there seems to be an optimum particle size required for FTS. With increasing particle size, CO adsorption of Fe/Al_2O_3 catalyst decreases and iron dispersion decreases at the surface of support, whereas the reduction degree increases with the increase of particle size. The catalytic activity of sample 200-5Fe/Al (particle size 6.1 nm) is found to be the best suited for FTS in the present studies. The CO conversion in the FTS was dependent on particle size, and hydrocarbon selectivities were strongly affected by the particle size for catalysts in the size range of 2.0–12.0 nm. At 300 °C, TOF increases from 0.06 to 0.187 s^{-1} when the particle size of the reduced catalyst is increased from 2.0 to 6.1 nm. It can therefore be concluded that particle size of iron oxide seems to be important for the catalytic activity and selectivity of Fe/Al_2O_3 catalysts.

Acknowledgements

The authors would like to acknowledge the financial support from the Korea Ministry of Knowledge Economy (MKE) through "Project of next-generation novel technology development" of ITEP. Dr. P.K. Khanna is thankful to Korea Federation of Science & Technology (KOSEF) for giving Brain-Pool fellowship.

References

[1] G.L. Bezemer, J.H. Bitter, H.P.C.E. Kuipers, H. Oosterbeek, J.E. Holewijn, X. Xu, F. Kapteijn, A.J. van Dillen, K.P. de Jong, J. Am. Chem. Soc. 128 (2006) 3956.
[2] J.P. den Breejen, P.B. Radstake, G.L. Bezemer, J.H. Bitter, V. Frøseth, A. Holmen, K.P. de Jong, J. Am. Chem. Soc. 131 (2009) 7197.
[3] J. Gaube, H.-F. Klein, J. Mol. Catal. A: Chem. 283 (2008) 60.
[4] B.H. Davis, Catal. Today 141 (2009) 25.
[5] M. Luo, R. O'Brien, B.H. Davis, Catal. Lett. 98 (2004) 17.
[6] E. Iglesia, S.L. Soled, R.A. Fiato, J. Catal. 137 (1992) 212.
[7] R. Oukaci, A.H. Singleton, J.G. Goodwin, Appl. Catal. A 186 (1999) 129.
[8] R.C. Reuel, C.H. Bartholomew, J. Catal. 85 (1984) 78.
[9] A. Martinez, C. Lopez, F. Marquez, I. Diaz, J. Catal. 220 (2003) 486.
[10] A.M. Saib, M. Claeys, E. van Steen, Catal. Today 71 (2002) 395.
[11] Y.-J. Lee, J.-Y. Park, K.-W. Jun, J.W. Bae, P.S. Sai Prasad, Catal. Lett. 130 (2009) 198.
[12] S.-H. Kang, J.W. Bae, P.S. Sai Prasad, K.-W. Jun, Catal. Lett. 125 (2008) 264.
[13] G. Prieto, A. Martínez, P. Concepción, R. Moreno-Tost, J. Catal. 266 (2009) 129.
[14] E.I. Mabaso, E. van Steen, M. Claeys, DGMK Tagungsbericht 4 (2006) 93.
[15] V.K. Jones, L.R. Neubauer, C.H. Bartholomew, J. Phys. Chem. 90 (1986) 4832.
[16] M.E. Dry, in: J. Anderson, M. Boudart (Eds.), Catalysis Science & Technology, vol. 1, Springer-Verlag, Berlin, 1981, p. 160.
[17] D.B. Bukur, L. Nowicki, R.K. Manne, X.S. Lang, J. Catal. 155 (1995) 366.
[18] R.M.M. Abbaslou, A. Tavasoli, A.K. Dalai, Appl. Catal. A 355 (2009) 33.
[19] J.F. Bengoa, A.M. Alvarez, M.V. Cagnoli, N.G. Gallegos, S.G. Marchetti, Appl. Catal. A 325 (2007) 68.
[20] Z. Tao, Y. Yang, M. Ding, T. Li, H. Xiang, Y. Li, Catal. Lett. 117 (2007) 130.
[21] G.B. Raupp, W.N. Delgass, J. Catal. 58 (1979) 337.
[22] M.V. Cagnoli, S.G. Marchett, N.G. Gallegos, A.M. Alvarez, A.A. Yeramián, R.C. Mercader, J. Catal. 123 (1990) 21.
[23] Y.-J. Lee, K.-W. Jun, J.-Y. Park, H.S. Potdar, R.C. Chikate, J. Ind. Eng. Chem. 14 (2008) 38.
[24] S.M. Kim, Y.-J. Lee, K.-W. Jun, J.-Y. Park, H.S. Potdar, Mater. Chem. Phys. 104 (2007) 56.
[25] T. Taniguchi, K. Nakagawa, T. Watanabe, N. Matsushita, M. Yoshimura, J. Phys. Chem. C 113 (2009) 839.
[26] Z. Jing, S. Wu, Mater. Lett. 58 (2006) 3637.
[27] Z. Jing, D. Han, S. Wu, Mater. Lett. 59 (2005) 804.
[28] Y. Jin, A.K. Datye, J. Catal. 196 (2000) 8.
[29] C.-H. Zhang, H.-J. Wan, Y. Yang, H.-W. Xiang, Y.-W. Li, Catal. Commun. 7 (2006) 733.
[30] H.-J. Wan, B.-S. Wu, C.-H. Zhang, H.-W. Xiang, Y.-W. Li, B.-F. Xu, F. Yi, Catal. Commun. 8 (2007) 1538.
[31] H.B. Zhang, G.L. Schrader, J. Catal. 95 (1985) 325.
[32] N.G. Gallegos, A.M. Alvarez, M.V. Cagnoli, J.F. Bengoa, S.G. Marchetti, R.C. Mercader, A.A. Yeramian, J. Catal. 161 (1996) 132.
[33] E. van Steen, M. Claeys, M.E. Dry, J. van de Loosdrecht, E.L. Viljoen, J.L. Visagie, J. Phys. Chem. B 109 (2005) 3575.
[34] R.A. Van Santen, Acc. Chem. Res. 42 (2009) 57.